MEASURING PRIMORDIAL NON-GAUSSIANITY IN THE COSMIC MICROWAVE BACKGROUND

E. Komatsu[1], D. N. Spergel[1], B. D. Wandelt[2]

komatsu@astro.princeton.edu

May 12, 2003

ABSTRACT

We derive a fast way for measuring primordial non-Gaussianity in a nearly full-sky map of the cosmic microwave background. We find a cubic combination of sky maps combining bispectrum configurations to capture a quadratic term in primordial fluctuations. Our method takes only $N^{3/2}$ operations rather than $N^{5/2}$ of the bispectrum analysis (1000 times faster for $l = 512$), retaining the same sensitivity. A key component is a map of underlying primordial fluctuations, which can be more sensitive to the primordial non-Gaussianity than a temperature map. We also derive a fast and accurate statistic for measuring non-Gaussian signals from foreground point sources. The statistic is 10^6 times faster than the full bispectrum analysis, and can be used to estimate contamination from the sources. Our algorithm has been successfully applied to the *Wilkinson Microwave Anisotropy Probe* sky maps by Komatsu et al. (2003).

Subject headings: cosmic microwave background — cosmology: observations — early universe

1. INTRODUCTION

Measurement of statistical properties of the cosmic microwave background (CMB) is a direct test of inflation. Simple models of inflation predict Gaussian primordial fluctuations generated by ground-state quantum fluctuations of a scalar field (Guth & Pi 1982; Starobinsky 1982; Hawking 1982; Bardeen et al. 1983; Mukhanov et al. 1992).

Non-linearity (Salopek & Bond 1990, 1991; Gangui et al. 1994; Gupta et al. 2002), interactions of scalar fields (Allen et al. 1987; Falk et al. 1993), or deviation from the ground state (Lesgourgues et al. 1997; Martin et al. 2000; Contaldi et al. 1999; Gangui et al. 2002) can generate weak non-Gaussianity. Acquaviva et al. (2002) and Maldacena (2002) have calculated the

[1]Department of Astrophysical Sciences, Princeton University, Princeton, NJ 08544

[2]Department of Physics, University of Illinois at Urbana-Champaign, Urbana, IL 61801-3080

2nd-order perturbations during inflation to show that simple inflation based on a slowly rolling scalar field cannot generate detectable non-Gaussianity with the *Wilkinson Microwave Anisotropy Probe* (*WMAP*) or the *Planck* experiments; thus, any detection of the primordial non-Gaussianity strongly constrains inflation models, and sheds light on physics in the early universe. For example, isocurvature fluctuations (Linde & Mukhanov 1997; Peebles 1997; Bucher & Zhu 1997), features in a scalar-field potential (Kofman et al. 1991; Wang & Kamionkowski 2000), or a "curvaton" mechanism (by which late-time decay of a scalar field generates curvature perturbations from isocurvature fluctuations (Mollerach 1990; Lyth & Wands 2002)) can generate stronger, potentially detectable, non-Gaussianity. The second-order gravity also contributes to non-Gaussianity (Luo & Schramm 1993; Munshi et al. 1995; Pyne & Carroll 1996; Mollerach & Matarrese 1997), and there is a possibility that we can detect it with the *Planck* experiment.

Many of the non-Gaussian models are written as a parametrized form for the curvature perturbations Φ,

$$\Phi(\boldsymbol{x}) = \Phi_L(\boldsymbol{x}) + f_{NL}\left[\Phi_L^2(\boldsymbol{x}) - \left\langle \Phi_L^2(\boldsymbol{x})\right\rangle\right], \tag{1}$$

where Φ_L are Gaussian linear perturbations. Note that $\Phi = \Phi_H$ in Bardeen (1980). A similar model may also apply to isocurvature perturbations, S (Bartolo et al. 2002). This *ansatz* provides a model quantifying the amplitude of the primordial non-Gaussianity. An exact prediction of this model for the CMB bispectrum exists (Komatsu & Spergel 2001), while an approximate one for the trispectrum (Okamoto & Hu 2002). Non-linearity in inflation gives $f_{NL} \sim \mathcal{O}(10^{-1})$, the second-order gravity gives $f_{NL} \gtrsim \mathcal{O}(1)$, and isocurvature fluctuations, features, or curvatons can give $f_{NL} \gg 1$ depending on models.

The bispectrum measured by *COBE* (Komatsu et al. 2002) and *MAXIMA* (Santos et al. 2002) experiments found $|f_{NL}| \lesssim 10^3$ (68%). Using the methods described in this paper, the *WMAP* data (Bennett et al. 2003b) have improved the constraint significantly to obtain $-58 < f_{NL} < 134$ (95%) (Komatsu et al. 2003). While the trispectrum measured on the *COBE* data has shown no evidence for cosmological non-Gaussianity (Komatsu 2001; Kunz et al. 2001), no quantitative limit on f_{NL} has been obtained. The trispectrum can be as sensitive to f_{NL} as the bispectrum (Okamoto & Hu 2002); however, we need more accurate predictions using the full radiation transfer function. The trispectrum has not yet been measured on the *WMAP* data. The deficit in $C^2(\theta)$ on $\theta \gtrsim 60^\circ$ (Spergel et al. 2003) might be a sign of a significant trispectrum on large angular scales.

Measuring f_{NL} from nearly full-sky experiments is challenging. The bispectrum analysis requires $N^{5/2}$ operations ($N^{3/2}$ for computing three l's and N for averaging over the sky) where N is the number of pixels ($N \sim 3 \times 10^6$ for *WMAP*, 5×10^7 for *Planck*). Even though an efficient algorithm exists, the trispectrum still requires N^3 (Komatsu 2001).

Although we measure the individual triangle configurations of the bispectrum (or quadrilateral configurations of the trispectrum) at first, we eventually combine all of them to constrain model parameters such as f_{NL}, as the signal-to-noise per configuration is nearly zero. This may sound inefficient. Measuring all configurations is enormously time consuming. Is there any statistic which *already* combines all the configurations optimally, and fast to compute? Yes, and finding it is the main subject of this paper. A physical justification for our methodology is as follows. A model like equation (1) generates non-Gaussianity in real space, and central-limit theorem makes the Fourier modes nearly Gaussian; thus, real-space statistics should be more sensitive. On the other hand, real-space statistics are weighted sum of Fourier-space statistics, which are often easier to predict. Therefore, we need to understand the shape of Fourier-space statistics to find sensitive real-space statistics, and for this purpose it is useful to have a specific, physically motivated non-Gaussian model, compute Fourier statistics, and find optimal real-space statistics.

2. RECONSTRUCTING PRIMORDIAL FLUCTUATIONS FROM TEMPERATURE ANISOTROPY

We begin with the primordial curvature perturbations $\Phi\left(\boldsymbol{x}\right)$ and isocurvature perturbations $S\left(\boldsymbol{x}\right)$. If we can reconstruct these primordial fluctuations from observed CMB anisotropy, $\Delta T(\hat{\boldsymbol{n}})/T$, then we can improve sensitivity to primordial non-Gaussianity. We find that the harmonic coefficients of CMB anisotropy, $a_{lm} = T^{-1}\int d^2\hat{\mathbf{n}}\Delta T(\hat{\boldsymbol{n}})Y_{lm}^*(\hat{\boldsymbol{n}})$, are related to the primordial fluctuations as

$$a_{lm} = b_l \int r^2 dr \left[\Phi_{lm}(r)\alpha_l^{adi}(r) + S_{lm}(r)\alpha_l^{iso}(r)\right] + n_{lm}, \tag{2}$$

where $\Phi_{lm}(r)$ and $S_{lm}(r)$ are the harmonic coefficients of the fluctuations at a given comoving distance, $r = |\boldsymbol{x}|$. A beam function b_l and the harmonic coefficients of noise n_{lm} represent instrumental effects. Since noise can be spatially inhomogeneous, the noise covariance matrix $\left\langle n_{lm}n_{l'm'}^*\right\rangle$ can be non-diagonal; however, we approximate it with $\simeq \sigma_0^2\delta_{ll'}\delta_{mm'}$. We thus assume the "mildly inhomogeneous" noise for which this approximation holds. The function $\alpha_l(r)$ is defined by

$$\alpha_l(r) \equiv \frac{2}{\pi}\int k^2 dk g_{Tl}(k) j_l(kr), \tag{3}$$

where $g_{Tl}(k)$ is the radiation transfer function of either adiabatic (*adi*) or isocurvature (*iso*) perturbations.

Next, assuming that $\Phi\left(\boldsymbol{x}\right)$ dominates, we try to reconstruct $\Phi\left(\boldsymbol{x}\right)$ from the observed $\Delta T(\hat{\boldsymbol{n}})$. A linear filter, $\mathcal{O}_l(r)$, which reconstructs the underlying field, can be obtained by minimizing variance of difference between the filtered field $\mathcal{O}_l(r)a_{lm}$ and the underlying field $\Phi_{lm}(r)$. By evaluating

$$\frac{\partial}{\partial \mathcal{O}_l(r)}\left\langle \left|\mathcal{O}_l(r)a_{lm} - \Phi_{lm}(r)\right|^2\right\rangle = 0, \tag{4}$$

one obtains a solution for the filter as

$$\mathcal{O}_l(r) = \frac{\beta_l(r) b_l}{\mathcal{C}_l}, \tag{5}$$

where the function $\beta_l(r)$ is given by

$$\beta_l(r) \equiv \frac{2}{\pi}\int k^2 dk P(k) g_{Tl}(k) j_l(kr), \tag{6}$$

and $P(k)$ is the power spectrum of Φ. Of course, one can replace Φ with S when S dominates. We use a calligraphic letter for a quantity that includes effects of b_l and noise such that $\mathcal{C}_l \equiv C_l b_l^2 + \sigma_0^2$, where C_l is the theoretical power spectrum that uses the same cosmological model as $g_{Tl}(k)$.

Finally, we transform the filtered field $\mathcal{O}_l(r)a_{lm}$ back to pixel space to obtain an Wiener-filtered, reconstructed map of $\Phi(r,\hat{\boldsymbol{n}})$ or $S(r,\hat{\boldsymbol{n}})$. We have assumed that there is no correlation between Φ and S. We will return to study the case of non-zero correlation later (§ 3.2).

Figure 1 shows $\mathcal{O}_l(r)$ as a function of l and r for (a) an adiabatic SCDM ($\Omega_m = 1$), (b) an adiabatic ΛCDM ($\Omega_m = 0.3$), (c) an isocurvature SCDM, and (d) an isocurvature ΛCDM. While we have used $P(k) \propto k^{-3}$ for both adiabatic and isocurvature modes, specific choice of $P(k)$ does not affect $\mathcal{O}_l$ very much as $P(k)$ in β_l in the numerator approximately cancels out $P(k)$ in $\mathcal{C}_l$ in the denominator. On large angular scales (smaller l) the Sachs–Wolfe (SW) effect makes $\mathcal{O}_l$ -3 for adiabatic modes and $-5/2$ for isocurvature modes of the SCDM models (Sachs & Wolfe 1967). For the ΛCDM models the late-time decay of gravitational potential makes this limit different. Adiabatic and isocurvature modes are out of phases in l.

The figure shows that $\mathcal{O}_l$ changes the sign of the fluctuations as a function of scales. This indicates that acoustic physics at the last scattering surface modulates fluctuations so that hot spots in the primordial fluctuations can be cold spots in CMB for example. Therefore, the shape of $\mathcal{O}_l$ "deconvolves" the sign change, recovering the phases of fluctuations. This is an intuitive reason why our cubic statistic derived below [Eq. (9)] works, and it proves more advantageous to measure primordial non-Gaussianity on a filtered map than on a temperature map.

This property should be compared to that of real-space statistics measured on a temperature map. We have shown in Komatsu & Spergel (2001) that the skewness of a temperature map is much less sensitive to the primordial non-Gaussianity than the bispectrum, exactly because of the cancellation effect from the acoustic oscillations. The skewness of a filtered map, on the other hand, has a larger signal-to-noise ratio, and a more optimal statistic like our cubic statistic derived below (§ 3) can be constructed. Other real-space statistics such as Minkowski functionals or peak-peak correlations may also be more sensitive to the primordial non-Gaussianity, when measured on the filtered maps; we are investigating these possibilities.

Unfortunately, as g_{Tl} oscillates, our reconstruction of Φ or S from a temperature map alone is not perfect. While $\mathcal{O}_l$ reconstructs the primordial fluctuations very well on large scales via the Sachs–Wolfe effect, $\mathcal{O}_l \sim 0$ on intermediate scales ($l \sim 50$ for adiabatic and $l \sim 100$ for isocurvature), indicating loss of information on the phases of the underlying fluctuations. Then, toward smaller scales, we recover information, lose information, and so on. Exact scales at which $\mathcal{O}_l \sim 0$ depend on r and cosmology. A good news is that a high signal-to-noise map of the CMB polarization anisotropy will enable us to overcome the loss of information, as the polarization transfer function is out of phases in l compared to the temperature transfer function, filling up information at which $\mathcal{O}_l \sim 0$. In the other words, the polarization anisotropy has finite information about the phases of the primordial perturbations, when the temperature anisotropy has zero information.

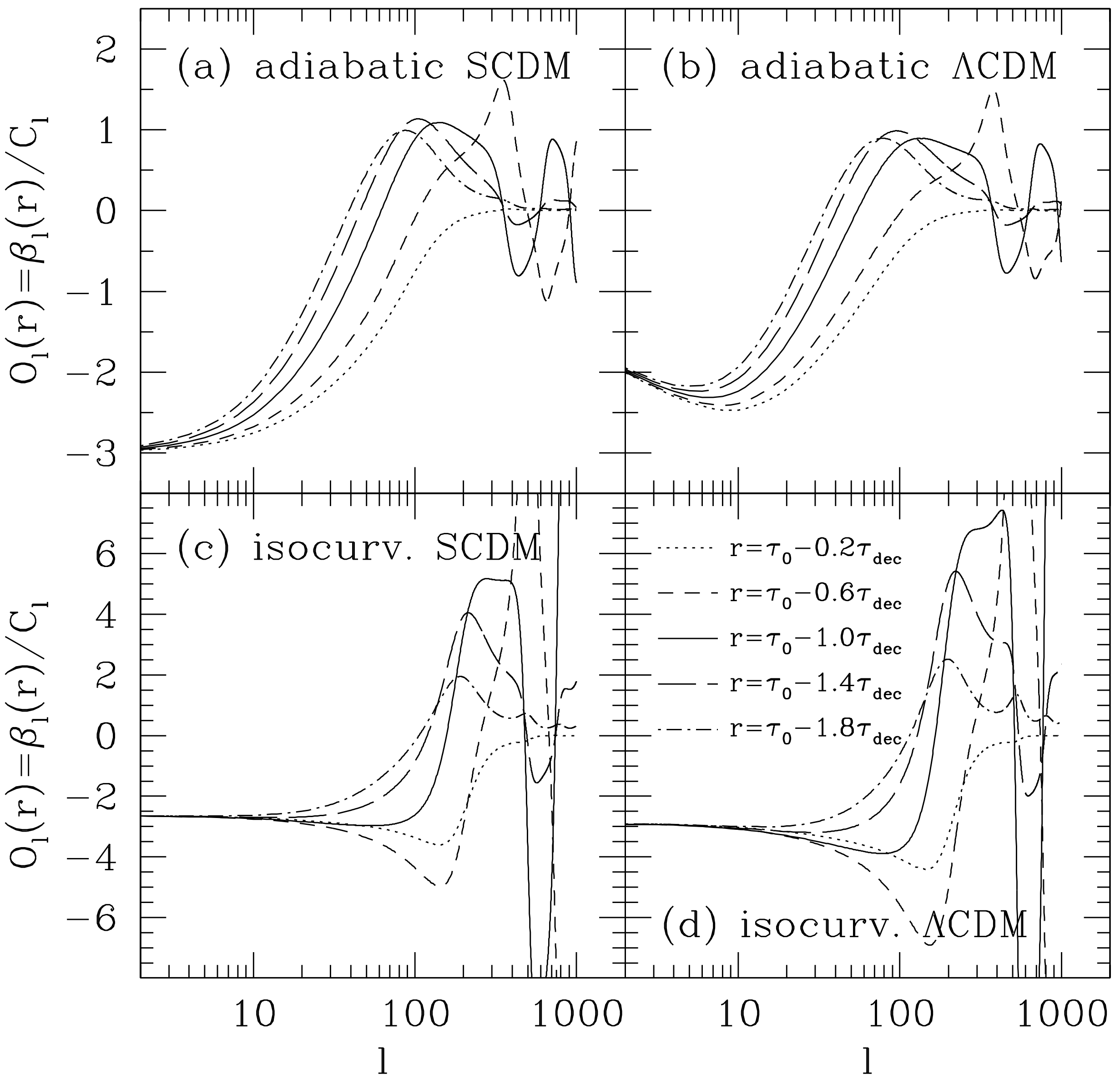

Fig. 1.— Wiener filters for the primordial fluctuations applied to a CMB sky map, $\mathcal{O}_l(r) = \beta_l(r)/C_l$ [Eq. (5)]. We plot (a) $\mathcal{O}_l$ for an adiabatic SCDM ($\Omega_m = 1$, $\Omega_\Lambda = 0$, $\Omega_b = 0.05$, $h = 0.5$), (b) for an adiabatic ΛCDM ($\Omega_m = 0.3$, $\Omega_\Lambda = 0.7$, $\Omega_b = 0.04$, $h = 0.7$), (c) for an isocurvature SCDM, and (d) for an isocurvature ΛCDM. The filters are plotted at five conformal distances $r = c(\tau_0 - \tau)$ as explained in the bottom-right panel. Here τ is the conformal time (τ_0 at the present). The SCDM models have $c\tau_0 = 11.84$ Gpc and $c\tau_{dec} = 0.235$ Gpc, while the ΛCDM models $c\tau_0 = 13.89$ Gpc and $c\tau_{dec} = 0.277$ Gpc, where τ_{dec} is the photon decoupling epoch.

3. FAST CUBIC STATISTICS

3.1. Primordial Non-Gaussianity

Using two functions introduced in the previous section, we construct a *cubic* statistic optimal for the primordial non-Gaussianity. We apply filters to a_{lm}, and then transform the filtered a_{lm}'s to obtain two maps, A and B, given by

$$A(r, \hat{\boldsymbol{n}}) \equiv \sum_{lm} \frac{\alpha_l(r) b_l}{\mathcal{C}_l} a_{lm} Y_{lm}(\hat{\boldsymbol{n}}), \tag{7}$$

$$B(r, \hat{\boldsymbol{n}}) \equiv \sum_{lm} \frac{\beta_l(r) b_l}{\mathcal{C}_l} a_{lm} Y_{lm}(\hat{\boldsymbol{n}}). \tag{8}$$

The latter map, $B(r, \hat{\boldsymbol{n}})$, is exactly the $\mathcal{O}_l$-filtered map, an Wiener-filtered map of the underlying primordial fluctuations. We then form a cubic statistic given by

$$\mathcal{S}_{prim} \equiv 4\pi \int r^2 dr \int \frac{d^2\hat{\boldsymbol{n}}}{4\pi} A(r, \hat{\boldsymbol{n}}) B^2(r, \hat{\boldsymbol{n}}), \tag{9}$$

where the angular average is done on full sky regardless of sky cut. We find that $\mathcal{S}_{prim}$ reduces *exactly* to

$$\mathcal{S}_{prim} = \sum_{l_1 \le l_2 \le l_3} \frac{\mathcal{B}^{obs}_{l_1 l_2 l_3} \mathcal{B}^{prim}_{l_1 l_2 l_3}}{\mathcal{C}_{l_1} \mathcal{C}_{l_2} \mathcal{C}_{l_3}}, \tag{10}$$

where

$$\mathcal{B}_{l_1 l_2 l_3} \equiv B_{l_1 l_2 l_3} b_{l_1} b_{l_2} b_{l_3}, \tag{11}$$

and $B^{obs}_{l_1 l_2 l_3}$ is the observed bispectrum with the effect of b_l corrected while $B^{prim}_{l_1 l_2 l_3}$ the theoretical one for $f_{NL} = 1$ (Komatsu & Spergel 2001),

$$B^{prim}_{l_1 l_2 l_3} \equiv 2 I_{l_1 l_2 l_3} \int r^2 dr \left[\beta_{l_1}(r) \beta_{l_2}(r) \alpha_{l_3}(r) + \beta_{l_3}(r) \beta_{l_1}(r) \alpha_{l_2}(r) + \beta_{l_2}(r) \beta_{l_3}(r) \alpha_{l_1}(r) \right], \tag{12}$$

where

$$I_{l_1 l_2 l_3} \equiv \sqrt{\frac{(2l_1+1)(2l_2+1)(2l_3+1)}{4\pi}} \begin{pmatrix} l_1 & l_2 & l_3 \\ 0 & 0 & 0 \end{pmatrix}. \tag{13}$$

It is straightforward to derive equation (10) from (9) using equation (12).

The denominator of equation (10) is the variance of $\mathcal{B}^{obs}_{l_1 l_2 l_3}$ in the limit of weak non-Gaussianity (say $|f_{NL}| \lesssim 10^3$) when all l's are different: $\left\langle \mathcal{B}^2_{l_1 l_2 l_3} \right\rangle = \mathcal{C}_{l_1} \mathcal{C}_{l_2} \mathcal{C}_{l_3} \Delta_{l_1 l_2 l_3}$, where $\Delta_{l_1 l_2 l_3}$ is 6 for $l_1 = l_2 = l_3$, 2 for $l_1 = l_2 \neq l_3$ etc., and 1 otherwise. The bispectrum configurations are thus summed up nearly optimally with the approximate inverse-variance weights, provided that $\Delta_{l_1 l_2 l_3}$ is approximated with $\simeq 1$. The least-square fit of $\mathcal{B}^{prim}_{l_1 l_2 l_3}$ to $\mathcal{B}^{obs}_{l_1 l_2 l_3}$ can be performed to yield

$$\mathcal{S}_{prim} \simeq f_{NL} \sum_{l_1 \le l_2 \le l_3} \frac{(\mathcal{B}^{prim}_{l_1 l_2 l_3})^2}{\mathcal{C}_{l_1} \mathcal{C}_{l_2} \mathcal{C}_{l_3}}. \tag{14}$$

This equation gives an estimate of f_{NL} directly from $\mathcal{S}_{prim}$.

The most time consuming part is the back-and-forth harmonic transformation necessary for pre-filtering [Eqs. (7) and (8)], taking $N^{3/2}$ operations times the number of sampling points of r, of order 100, for evaluating the integral [Eq. (9)]. This is much faster than the full bispectrum analysis which takes $N^{5/2}$, enabling us to perform a more detailed analysis of the data in a reasonable amount of computational time. For example, measurements of all bispectrum configurations up to $l_{max} = 512$ take 8 hours to compute on 16 processors of an SGI Origin 300; thus, even only 100 Monte Carlo simulations take 1 month to carry out. On the other hand, $\mathcal{S}_{prim}$ takes only 30 seconds to compute, 1000 times faster. When we measure f_{NL} for $l_{max} = 1024$, we speed up by a factor of 4000: 11 days for the bispectrum vs 4 minutes for $\mathcal{S}_{prim}$. We can do 1000 simulations for $l_{max} = 1024$ in 3 days.

3.2. Mixed Fluctuations

The $\mathcal{O}_l$-filtered map, B, is an Wiener-filtered map of primordial curvature or isocurvature perturbations; however, this is correct only when correlations between the two components are negligible. On the other hand, multi-field inflation models (Langlois 1999; Gordon et al. 2001) and curvaton models (Lyth & Wands 2002; Moroi & Takahashi 2001) naturally predict correlations. The current CMB data are consistent with, but do not require, a mixture of the correlated fluctuations (Amendola et al. 2002; Trotta et al. 2001; Peiris et al. 2003). In this case, the Wiener filter for the primordial fluctuations [Eq. (5)] needs to be modified such that $\mathcal{O}_l(r) = \beta_l(r) b_l/\mathcal{C}_l \rightarrow \tilde{\beta}_l(r) b_l/\mathcal{C}_l$, where

$$\begin{aligned}
\tilde{\beta}_l^{adi}(r) &= \frac{2}{\pi}\int k^2 dk \left[P_\Phi(k) g_{Tl}^{adi}(k) + P_C(k) g_{Tl}^{iso}(k)\right] j_l(kr), \\
\tilde{\beta}_l^{iso}(r) &= \frac{2}{\pi}\int k^2 dk \left[P_S(k) g_{Tl}^{iso}(k) + P_C(k) g_{Tl}^{adi}(k)\right] j_l(kr),
\end{aligned}$$

for curvature (adi) and isocurvature (iso) perturbations, respectively. Here P_Φ is the primordial power spectrum of curvature perturbations, P_S of isocurvature perturbations, and P_C of cross correlations.

As for measuring non-Gaussianity from the correlated fluctuations, we use equation (1) as a model of Φ- and S-field non-Gaussianity to parameterize them with f_{NL}^{adi} and f_{NL}^{iso}, respectively. We then form a cubic statistic similar to $\mathcal{S}_{prim}$ [Eq. (9)], using $A(r, \hat{\boldsymbol{n}})$ and a new filtered map $\tilde{B}(r, \hat{\boldsymbol{n}})$ which uses $\tilde{\beta}_l(r)$. We have two cubic combinations: $A_{adi}\tilde{B}_{adi}^2$ for measuring f_{NL}^{adi} and $A_{iso}\tilde{B}_{iso}^2$ for f_{NL}^{iso}, each of which comprises four terms including one P_Φ^2 (or P_S^2), one P_C^2, and two $P_\Phi P_C$'s (or $P_S P_C$'s). In other words, the correlated contribution makes the total number of terms contributing to the non-Gaussianity four times more than the uncorrelated-fluctuation models (see (Bartolo et al. 2002) for more generic cases).

3.3. Point Source Non-Gaussianity

Next, we show that the filtering method is also useful for measuring foreground non-Gaussianity arising from extragalactic point sources. The residual point sources left unsubtracted in a map can seriously contaminate both the power spectrum and the bispectrum. We can, on the other hand, use multi-band observations as well as external template maps of dust, free-free, and synchrotron emission, to remove diffuse Galactic foreground (Bennett et al. 2003a). The radio sources with known positions can be safely masked.

The filtered map for the point sources is

$$D(\hat{\boldsymbol{n}}) \equiv \sum_{lm} \frac{b_l}{\mathcal{C}_l} a_{lm} Y_{lm}(\hat{\boldsymbol{n}}). \tag{15}$$

This filtered map was actually used for detecting point sources in the *WMAP* maps (Bennett et al. 2003a). Using $D(\hat{\boldsymbol{n}})$, the cubic statistic is derived as

$$\mathcal{S}_{src} \equiv \int \frac{d^2\hat{\boldsymbol{n}}}{4\pi} D^3(\hat{\boldsymbol{n}}) = \frac{3}{2\pi} \sum_{l_1 \le l_2 \le l_3} \frac{\mathcal{B}^{obs}_{l_1 l_2 l_3} \mathcal{B}^{src}_{l_1 l_2 l_3}}{\mathcal{C}_{l_1} \mathcal{C}_{l_2} \mathcal{C}_{l_3}}. \tag{16}$$

Here, $B^{src}_{l_1 l_2 l_3}$ is the point-source bispectrum for unit white-noise bispectrum, $B^{src}_{l_1 l_2 l_3} = I_{l_1 l_2 l_3}$. ($b_{src} = 1$ in Komatsu & Spergel (2001).) When covariance between $B^{prim}_{l_1 l_2 l_3}$ and $B^{src}_{l_1 l_2 l_3}$ is negligible as is the case for *WMAP* and *Planck* (Komatsu & Spergel 2001), we find

$$\mathcal{S}_{src} \simeq \frac{3 b_{src}}{2\pi} \sum_{l_1 \le l_2 \le l_3} \frac{(\mathcal{B}^{src}_{l_1 l_2 l_3})^2}{\mathcal{C}_{l_1} \mathcal{C}_{l_2} \mathcal{C}_{l_3}}. \tag{17}$$

We omit the covariance only for simplicity; including it is simple (Komatsu & Spergel 2001; Komatsu et al. 2002). Again $\mathcal{S}_{src}$ measures b_{src} much faster than the full bispectrum analysis, constraining effects of residual point sources on CMB sky maps. Since $\mathcal{S}_{src}$ does not contain the extra integral over r, it is even 100 times faster to compute than $\mathcal{S}_{prim}$. This statistic is particularly useful because it is sometimes difficult to tell how much of C_l is due to point sources. Komatsu et al. (2003) have used $\mathcal{S}_{src}$ (i.e., b_{src}) to measure C_l due to the unsubtracted point sources.

3.4. Incomplete Sky Coverage

Finally, we show how to incorporate incomplete sky coverage and pixel weights into our statistics. Suppose that we weight a sky map by $M(\hat{\boldsymbol{n}})$ to measure the harmonic coefficients,

$$a^{obs}_{lm} = T^{-1} \int d^2\hat{\boldsymbol{n}} M(\hat{\boldsymbol{n}}) \Delta T(\hat{\boldsymbol{n}}) Y^*_{lm}(\hat{\boldsymbol{n}}). \tag{18}$$

A full-sky a_{lm} is related to a^{obs}_{lm} through the coupling matrix $M_{ll'mm'} \equiv \int d^2\hat{\boldsymbol{n}} M(\hat{\boldsymbol{n}}) Y^*_{lm}(\hat{\boldsymbol{n}}) Y_{l'm'}(\hat{\boldsymbol{n}})$ by $a^{obs}_{lm} = \sum_{l'm'} a_{l'm'} M_{ll'mm'}$. In this case the observed bispectrum is biased by a factor of

$\int d^2\hat{\boldsymbol{n}}M^3(\hat{\boldsymbol{n}})/(4\pi)$; thus, we need to divide S_{prim} and S_{ps} by this factor. If only sky cut is considered, then this factor is a fraction of the sky covered by observations (Komatsu et al. 2002).

We have carried out extensive Monte Carlo simulations of non-Gaussian sky maps computed with equation (2). Appendix A of Komatsu et al. (2003) describes the simulations in detail. We find that $\mathcal{S}_{prim}$ reproduces input f_{NL}'s accurately both on full sky and incomplete sky with modest Galactic cut and inhomogeneous noise expected for *WMAP*, i.e., the statistic is unbiased. We also find that the error of f_{NL} from $\mathcal{S}_{prim}$ is as small as that from the full bispectrum analysis. We cannot however make a sky cut very large, e.g., more than 50% of the sky, as for which the covariance matrix of $\mathcal{B}_{l_1l_2l_3}$ is no longer diagonal. The cubic statistic does not include the off-diagonal terms of the covariance matrix [see Eq. (10)]; however, it works fine for *WMAP* sky maps for which we can use more than 75% of the sky. Also, we have found that equation (17) correctly estimates b_{src} using simulated realizations of point sources (see Appendix B of Komatsu et al. (2003)).

4. CONCLUSION

Using the method described in this paper, we can measure non-Gaussian fluctuations in a nearly full-sky CMB map much faster than the full bispectrum analysis without loss of sensitivity. Our fast statistics allow us to carry out extensive Monte Carlo simulations characterizing effects of realistic noise properties of experiments, sky cut, foreground sources, and so on. A reconstructed map of the primordial fluctuations, which plays a key role in our method, potentially gives other real-space statistics more sensitivity to primordial non-Gaussianity. As we have shown our method can be applied to the primordial non-Gaussianity arising from inflation, gravity, or correlated isocurvature fluctuations, as well as the foreground non-Gaussianity from radio point sources, all of which can be important sources of non-Gaussian fluctuations on the forthcoming CMB sky maps.

REFERENCES

Acquaviva, V., Bartolo, N., Matarrese, S., & Riotto, A. 2002, preprint, astro-ph/0209156

Allen, T. J., Grinstein, B., & Wise, M. B. 1987, Phys. Lett., B197, 66

Amendola, L., Gordon, C., Wands, D., & Sasaki, M. 2002, Phys. Rev. Lett., 88, 211302

Bardeen, J. M. 1980, Phys. Rev., D22, 1882

Bardeen, J. M., Steinhardt, P. J., & Turner, M. S. 1983, Phys. Rev. D, 28, 679

Bartolo, N., Matarrese, S., & Riotto, A. 2002, Phys. Rev., D65, 103505

Bennett, C., Hill, R. S., Hinshaw, G., Nolta, M. R., Odegard, N., Page, L., Spergel, D. N., Weiland, J. L., Wright, E. L., Halpern, M., Jarosik, N., Kogut, A., Limon, M., Meyer, S. S., Tucker, G. S., & Wollack, E. 2003a, 2208, ApJ, submitted (astro-ph/0302208)

Bennett, C. L., Halpern, M., Hinshaw, G., Jarosik, N., Kogut, A., Limon, M., Meyer, S. S., Page, L., Spergel, D. N., Tucker, G. S., Wollack, E., Wright, E. L., Barnes, C., Greason, M. R., Hill, R. S., Komatsu, E., Nolta, M. R., Odegard, N., Peirs, H. V., Verde, L., & Weiland, J. L. 2003b, 2207, ApJ, submitted (astro-ph/0302207)

Bucher, M. & Zhu, Y. 1997, Phys. Rev., D55, 7415

Contaldi, C. R., Bean, R., & Magueijo, J. 1999, Phys. Lett., B468, 189

Falk, T., Rangarajan, R., & Srednicki, M. 1993, ApJ, 403, L1

Gangui, A., Lucchin, F., Matarrese, S., & Mollerach, S. 1994, ApJ, 430, 447

Gangui, A., Martin, J., & Sakellariadou, M. 2002, preprint, astro-ph/0205202

Gordon, C., Wands, D., Bassett, B. A., & Maartens, R. 2001, Phys. Rev., D63, 023506

Gupta, S., Berera, A., Heavens, A. F., & Matarrese, S. 2002, Phys. Rev., D66, 043510

Guth, A. H. & Pi, S.-Y. 1982, Phys. Rev. Lett., 49, 1110

Hawking, S. W. 1982, Phys. Lett., B115, 295

Kofman, L., Blumenthal, G. R., Hodges, H., & Primack, J. R. 1991, in ASP Conf. Ser. 15: Large-scale Structures and Peculiar Motions in the Universe, 339

Komatsu, E. 2001, ph.D. thesis at Tohoku University, astro-ph/0206039

Komatsu, E., Kogut, A., Nolta, M., Bennett, C. L., Halpern, M., Hinshaw, G., Jarosik, N., Limon, M., Meyer, S. S., Page, L., Spergel, D. N., Tucker, G. S., Verde, L., Wollack, E., & Wright, E. L. 2003, 2223, ApJ, submitted (astro-ph/0302223)

Komatsu, E. & Spergel, D. N. 2001, Phys. Rev. D, 63, 63002

Komatsu, E., Wandelt, B. D., Spergel, D. N., Banday, A. J., & Górski, K. M. 2002, ApJ, 566, 19

Kunz, M., Banday, A. J., Castro, P. G., Ferreira, P. G., & Górski, K. M. 2001, ApJ, 563, L99

Langlois, D. 1999, Phys. Rev., D59, 123512

Lesgourgues, J., Polarski, D., & Starobinsky, A. A. 1997, Nucl. Phys., B497, 479

Linde, A. D. & Mukhanov, V. 1997, Phys. Rev., D56, R535

Luo, X.-c. & Schramm, D. N. 1993, Phys. Rev. Lett., 71, 1124

Lyth, D. H. & Wands, D. 2002, Phys. Lett., B524, 5

Maldacena, J. 2002, preprint, astro-ph/0210603

Martin, J., Riazuelo, A., & Sakellariadou, M. 2000, Phys. Rev., D61, 083518

Mollerach, S. 1990, Phys. Rev., D42, 313

Mollerach, S. & Matarrese, S. 1997, Phys. Rev., D56, 4494

Moroi, T. & Takahashi, T. 2001, Phys. Lett., B522, 215

Mukhanov, V. F., Feldman, H. A., & Brandenberger, R. H. 1992, Phys. Rept., 215, 203

Munshi, D., Souradeep, T., & Starobinsky, A. A. 1995, ApJ, 454, 552

Okamoto, T. & Hu, W. 2002, Phys. Rev., D66, 063008

Peebles, P. J. E. 1997, ApJ, 483, L1

Peiris, H. V., Komatsu, E., Verde, L., Spergel, D. N., Bennett, C. L., Halpern, M., Hinshaw, G., Jarosik, N., Kogut, A., Limon, M., & Meyer, S. S. 2003, 2225, ApJ, submitted (astro-ph/0302225)

Pyne, T. & Carroll, S. M. 1996, Phys. Rev., D53, 2920

Sachs, R. K. & Wolfe, A. M. 1967, ApJ, 147, 73

Salopek, D. S. & Bond, J. R. 1990, Phys. Rev. D, 42, 3936

—. 1991, Phys. Rev. D, 43, 1005

Santos, M. G., Heavens, A., Balbi, A., Borrill, J., Ferreira, P. G., Hanany, S., Jaffe, A. H., Lee, A. T., Rabii, B., Richards, P. L., Smoot, G. F., Stompor, R., Winant, C. D., & Wu, J. H. P. 2002, 11123, preprint, astro-ph/0211123

Spergel, D. N., Verde, L., Peiris, H. V., Komatsu, E., Nolta, M. R., Bennett, C. L., Halpern, M., Hinshaw, G., Jarosik, N., Kogut, A., Limon, M., Meyer, S. S., Page, L., Tucker, G. S., Weiland, J. L., Wollack, E., & Wright, E. L. 2003, 2209, ApJ, submitted (astro-ph/0302209)

Starobinsky, A. A. 1982, Phys. Lett., B117, 175

Trotta, R., Riazuelo, A., & Durrer, R. 2001, Phys. Rev. Lett., 87, 231301

Wang, L.-M. & Kamionkowski, M. 2000, Phys. Rev., D61, 063504

This preprint was prepared with the AAS LaTeX macros v5.0.